Acta Histochemica xxx (2013) xxx–xxx

Contents lists available at ScienceDirect

Acta Histochemica

journal homepage: www.elsevier.de/acthis

Iron overload induces changes of pancreatic and duodenal divalent metal transporter 1 and prohepcidin expression in mice

Gisela Giorgi, Marta Elena Roque*

Laboratory of Human Physiology, Department of Biology, Biochemistry and Pharmacy, Universidad Nacional del Sur, San Juan 670, Bahía Blanca, Argentina

ARTICLE INFO

Article history:
Received 16 April 2013
Received in revised form 21 August 2013
Accepted 22 August 2013
Available online xxx

Keywords:
Divalent metal transporter 1
Prohepcidin
Ferritin
Iron overload
Pancreas
Mice

ABSTRACT

It is well known that the iron content of the body is tightly regulated. Iron excess induces adaptive changes that are differentially regulated in each tissue. The pancreas is particularly susceptible to iron-related disorders. We studied the expression and regulation of key iron proteins in the pancreas, duodenum and liver, using an animal model of iron overload (female CF1 mice injected i.p. with iron saccharate, colloidal iron form). Divalent metal transporter 1, prohepcidin and ferritin (pancreas, duodenum, liver) were assessed by immunohistochemistry; divalent metal transporter 1 (pancreas, duodenum) by Western blot. In the iron overloaded mice, prohepcidin expression increased in islets of Langerhans and hepatocytes, and divalent metal transporter 1 expression decreased in cells of islets and in enterocytes. In the iron overloaded mice, ferritin expression decreased in islets of Langerhans and increased in acinar cells; hemosiderin was localized in connective tissue cells. The inverse relationship between divalent metal transporter 1 and prohepcidin may indicate a negative regulation by hepcidin, and hence reduction of iron stores in islets of Langerhans. Our data showed that in iron overloaded mice model, induced by colloidal iron form, a coordinated expression of key iron proteins in the pancreas, duodenum and liver may occur. Further research will be necessary to determine the adaptive responses induced by iron in the pancreas.

Introduction

Over the last decade remarkable advances have been made in understanding iron metabolism. These studies led to the identification and characterization of novel proteins that interact with other well documented proteins such as ferritin and the transferrin proteins (Gkouvatsos et al., 2012). It is well known that iron homeostasis is maintained by a balance between iron uptake from the diet by duodenal enterocytes and by iron recycling from senescent erythrocytes in the reticuloendothelial system (Nicolas et al., 2001).

Hepcidin, the major regulator of iron stores, regulates cellular iron efflux by inducing ferroportin (FPN) degradation, the only iron exporter identified to date (Nemeth et al., 2004; D'Anna et al., 2009). Therefore in the presence of high hepcidin levels, iron efflux from FPN-expressing cells, such as enterocytes and macrophages, is significantly decreased (Chung et al., 2009).

Another key protein of iron metabolism is divalent metal transporter 1 (DMT1), involved in both iron uptake and release into the target cell. DMT1 is expressed at the apical membrane of duodenal enterocytes and in the endocytic compartment of peripheral tissues where it releases iron internalized throughout the transferrin system (Andrews, 1999). DMT1 has been studied in the duodenum where modulation of dietary iron absorption is the main mechanism for regulating body iron balance, noting that DMT1 expression is reduced when iron-rich foods are consumed, but increases when iron intake is restricted (Canonne-Hergaux et al., 1999). However in the liver, high levels of dietary iron produce an increase in DMT1 expression in hepatocytes, promoting iron acquisition, whereas low levels of iron decrease hepatic DMT1 expression, causing a reduction in iron accumulation (Trinder et al., 2000).

As regards hepcidin, the essential role of this peptide in the maintenance of systemic iron balance has been demonstrated in mouse models (Ganz and Nemeth, 2006; D'Anna et al., 2011). Hepcidin production by the liver is modulated in response to several stimuli such as hypoxia, inflammation and iron overload (Lee and Beutler, 2009). It has been reported that mice lacking hepcidin expression develop systemic iron overload, a disorder characterized by severe iron overload in several organs, including the liver, heart, and pancreatic tissues (Ramey et al., 2007; Masaratana et al., 2011). The iron storage proteins are ferritin, the primary intracellular iron-storage protein, and hemosiderin, a pigment protein produced by ferritin degradation (Iancu, 2011).

Although it is well known that hepcidin is mainly synthesized in hepatocytes (Park et al., 2001), several studies have identified and characterized its synthesis in extra hepatic tissues, such as the pancreas and kidney (Kulaksiz et al., 2008; Veuthey et al., 2008).

* Corresponding author.
E-mail address: mroque@uns.edu.ar (M.E. Roque).

0065-1281/$ – see front matter © 2013 Elsevier GmbH. All rights reserved.
http://dx.doi.org/10.1016/j.acthis.2013.08.013

Previously, the indirect relationship between hepcidin and DMT1 in duodenal and renal tissue has been demonstrated (Veuthey et al., 2008; Mena et al., 2008; Chung et al., 2009). Moreover, the role of the hepcidin–ferroportin axis in the regulation of systemic iron balance is well established (De Domenico et al., 2011; D'Anna and Roque, 2013).

Recent studies have suggested that iron balance is maintained, not only by this systemic regulation, but also by mechanisms that regulate iron balance at the cellular level (Finberg, 2011). For example, mice harboring an intestinal-specific deletion of the HIF-2α subunit were found to exhibit decreased serum and liver iron levels, even though their hepatic hepcidin expression was markedly decreased (Mastrogiannaki et al., 2009). Studies by Vanoaica et al. (2010) using mice with intestine-specific deletion of ferritin H demonstrated that not only Hepcidin-DMT1 axis is important to regulate duodenal iron uptake, but also ferritin expression is essential to prevent excessive iron absorption.

It is well known that pancreatic tissue is particularly susceptible to iron-related disorders such as hemochromatosis and secondary iron overload (Beutler, 2006). Furthermore, previous studies have found that key proteins of iron balance, such as hepcidin, DMT1 and ferritin, are expressed in the pancreas (MacDonald et al., 1994; Koch et al., 2003; Kulaksiz et al., 2008). However, the regulation and function of these crucial proteins of iron cycle in the pancreas are not entirely clear.

The aim of this study was to clarify the effects of iron excess on pancreatic tissue, in terms of regulation of iron proteins, and its relation to tissues most studied such as duodenum and liver. Thus, the aim of the present study was to determine prohepcidin expression using an *in vivo* model of iron overload and its relationship with DMT1 and ferritin.

Materials and methods

Animals

The studies have been carried out with CF1 mice, a strain with preserved genetic variability and phenotypic stability (Oyarzabal and Rabasa, 1999). CF1 female mice (25 ± 5 g; three months old) were bred at the animal facility of the Universidad Nacional del Sur. The animals were kept in cages at controlled room temperature and humidity under standard conditions (12 h light-dark period) and were fed throughout on a standard diet with access to water *ad libitum*. The animals selected for the experiment were distributed in cages 10 days prior to the beginning of the study. According to the paired sample design used, the body weight of each mice pair was similar at the beginning of the study and was controlled throughout the study. The procedures followed are in line with the Guide for the Care and Use of Laboratory Animals of NIH (Committee on Care and Use of Laboratory Animals, 1996). Prior to the initiation of this study, the protocol was approved by the Institutional Committee on Experimental Animal Use and Care of the Universidad Nacional del Sur (ICEAUC).

Experimental design

Adult CF1 female mice were divided into two groups (9 mice per group) and were selected in pairs according to body weight as variable following a paired-sample design: (1) iron overloaded mice group; mice received an intraperitoneal injection every 2 days with 500 μl (dose 333.3 mg/kg) iron saccharate (catalog no. 311: Rivero Laboratory, Buenos Aires, Argentina) during 18 days (overall dose 3000 mg/kg) and (2) iron-adequate mice group; mice received an intraperitoneal (500 μl) injection with saline solution (0.9% NaCl) (Sanadrog, Buenos Aires, Argentina). 5 days prior to iron saccharate or saline solution administration, a blood sample (80 μL) was collected from each mouse to determine baseline hematology. Animals were anesthetized with isoflurane for blood collection (day 20) to determine hematological parameters and plasma iron.

Antibodies

Primary antibodies: rabbit anti-mouse DMT1 (Canonne-Hergaux et al., 1999) kindly provided by François Canonne-Hergaux, INSERM, France. Rabbit anti-mouse L-chain ferritin (RbαMoLF) (Santambrogio et al., 2000) kindly provided by Paolo Santambrogio from Istituto di Ricovero e Cura a Carattere Scientifico (IRCCS), Milan, Italy. Prohepcidin antibody (Valore and Ganz, 2008) was kindly provided by Tomas Ganz, UCLA, Los Angeles, CA, USA. Goat anti-mouse actin (Santa Cruz Biotechnology, Santa Cruz, CA, USA). Secondary antibodies: Donkey anti-goat labeled HRP (Santa Cruz Biotechnology); Goat anti-rabbit labeled HRP (Alpha Diagnostics, Owings Mills, MD, USA).

Immunohistochemical and histochemical technique

The animals were sacrificed by cervical dislocation (day 20). The duodenum, pancreas and liver were removed under sterile conditions by abdominal incision. Tissues samples from mice were fixed by immersion in fresh fixative solution (10% neutral buffered formalin, pH 7) (catalog no. 2000170200; Biopack, Buenos Aires, Argentina) and embedded in paraffin wax. Sections of 5 μm were cut and mounted on glass slides. Before labeling, sections were deparaffinized in xylene and rehydrated in a graded series of ethanol baths. Endogenous peroxidase activity in deparaffinized sections was blocked with 3% H_2O_2 (catalog no. 7258; Anedra, Buenos Aires, Argentina). Sections were then incubated in phosphate buffered saline (PBS), pH 7.1, for 10 min at room temperature. Incubation with the primary antibody diluted in PBS (pH 7.1) was carried out in a humid chamber for 1 h at room temperature for DMT1, and overnight at 4 °C for prohepcidin and L-ferritin immunodetection. Dilutions of antibodies were as follows: anti-DMT1 (pancreas 1:250 and gut 1:50), anti-prohepcidin (1:1000) and anti-L-ferritin (1:500). Following incubation with the primary antibody, tissues were washed with PBS, incubated with goat anti-rabbit IgG peroxidase coupled secondary antibody for 1 h at room temperature, and then re-washed with PBS. Subsequent localization of proteins was revealed by reaction with 3′-diaminobenzidine tetrahydrochloride (DAB) in solution (catalog no. K3468; Dako, Glostrup, Denmark). Immunostained sections were followed by Prussian blue staining for iron, counterstaining with nuclear red to identify immunostained proteins separately from hemosiderin (double staining). Finally, sections were dehydrated in ethanol and xylene and mounted with coverslips. Negative controls included incubation with PBS for anti-DMT1 and anti-L-ferritin detection or pre-immune serum for anti-prohepcidin detection instead of the primary antibody, in each experiment and tissue studied. Immunostaining was analyzed using an Olympus BX51 microscope, equipped with ×10, ×20 and ×40 dry objectives, and an ×100 oil immersion objective. Digital images were obtained with an Olympus C7070 camera.

Prussian blue staining for iron was performed on sections of pancreas, duodenum and liver previously treated and non-treated with primary antibodies. Deparaffinized tissue sections were incubated in 2% HCl (catalog no. 6050: Anedra, Buenos Aires, Argentina) containing 10% potassium ferrocyanide for 15 min (catalog no. 104984: Merck Millipore, Buenos Aires, Argentina), washed and counterstained with nuclear red before visualization (catalog no. 1159390025: Merck Millipore, Buenos Aires, Argentina). We carried out the double staining (immunohistochemistry followed by

Please cite this article in press as: Giorgi G, Roque ME. Iron overload induces changes of pancreatic and duodenal divalent metal transporter 1 and prohepcidin expression in mice. Acta Histochemica (2013), http://dx.doi.org/10.1016/j.acthis.2013.08.013

Prussian blue) to identify immunostained proteins separately from hemosiderin pigments in the same tissue section.

Immunoblot analysis

For Western blot analysis ($n = 3$) proteins were extracted by homogenizing tissues at 4 °C in lysis buffer: 50 mM Tris-HCl (Tris buffer, cat. no. 166805; Biopak, Buenos Aires, Argentina); 150 mM NaCl (cat. no. 164607; Biopack, Buenos Aires, Argentina), 1 mM EDTA (catalog no. 160400; Biopack, Buenos Aires), 1% Tween-20 (cat. no.1979001; Wiener lab, Rosario, Argentina); 1% Triton X100 (cat. no. 9002-93-1; Sigma–Aldrich, Buenos Aires, Argentina); and protease inhibitor cocktail (cat. no. P2714; Sigma–Aldrich, St Louis, MO, USA). The homogenization was performed using an Ultra Turrax T8 homogenizer (IKA, Staufen, Germany) for 10 s. The homogenate was centrifuged at 10,000 *g* for 10 min at 4 °C. Protein concentration in the supernatant was determined by the Bradford method (Bradford, 1976). 100 μg (duodenal tissue) and 150 μg (pancreatic tissue) of protein was solubilized in Laemmli loading buffer and separated by SDS-PAGE on 10% acrylamide mix 30% (Acrylamide, cat. no. A5934: Sigma–Aldrich; bisacrylamide, catalog no. 294381: Sigma–Aldrich, Buenos Aires, Argentina); SDS 10% (cat. no. SB0485; Bio Basic A, Buenos Aires, Argentina); 1.5 M Tris-HCl (pH 8.8); ammonium persulfate 10% (catalog no. A9164; Sigma–Aldrich, Buenos Aires, Argentina); TEMED (cat. no. sc-29111; Santa Cruz Biotechnology). Then, proteins were transferred onto nitrocellulose membrane, blocked with 5% bovine serum albumin (BSA) (cat. no. sc-2323; Santa Cruz) in 0.1% Tween-20 in Tris-buffered saline (Tris-HCl 50 mM pH 7.4; NaCl 150 mM) for 1 h, and further incubated with rabbit anti-mouse DMT1 antibody overnight (1:500) at 4 °C. Immunoreactivity was observed using a horseradish peroxidase-linked secondary antibody goat anti-rabbit (cat. no. 20120; Alpha Diagnostic, San Antonio, TX, USA). As a housekeeping control we used goat anti-mouse actin antibody (catalog no. sc-2033; Santa Cruz Biotechnology), 1 h at room temperature. Immunoreactivity was observed using a horseradish peroxidase-linked secondary antibody (donkey anti-goat, cat. no. sc-2006, Santa Cruz Biotechnology). The blots were stripped between detection with different antibodies. Reactions were detected by enhanced chemiluminescence (ECL) following manufacturer's instructions (cat. no. 34077; Supersignal West Pico Chemiluminiscent substrate, Thermo Scientific). Membranes incubated in the absence of the primary antibody served as negative controls. Blots were scanned (HP Scanjet G3110) and processed with ImageJ software (ImageJ 1,47h, Wayne Rasband National Institute of Health, Bethesda, MD, USA).

Plasma and tissue iron quantification

Plasma samples from anticoagulated blood with heparin were obtained by centrifugation (Rolco, CH-24) at 15,000 rpm during 5 min. The iron levels were determined according to colorimetric ferrozine-based assay (Fer-Color, Wiener Lab). Liver and pancreas iron content was determined after acid digestion of tissue samples using nitric acid 35% (cat. no. 6112; Anedra, San Fernando, Argentina) followed by iron quantification with colorimetric ferrozine-based assay.

Hematology

Animals were anesthetized with isoflurane for blood collection from the retro-orbital venous plexus with heparinized capillaries, to determine hematological parameters: Hematocrit (microhematocrit method) and hemoglobin (cyanmethemoglobin method) (cat. no. 47WM Argentina, Buenos Aires, Argentina).

Table 1
Iron levels.

	Iron-adequate	Iron-overload
Pancreas (μmol/g wet tissue)	0.30 ± 0.19	106.96 ± 0.30**
Liver (μmol/g wet tissue)	0.96 ± 0.22	21.16 ± 5.86**
Plasma (μmol/dL)	264 ± 49	477 ± 108**

Results are expressed as means ± SD ($n = 9$).
** $p < 0.01$ iron-overloaded mice *vs.* iron-adequate mice.

Statistical analysis

In all mouse experiments, at least 9 mice were tested individually. Data were analyzed by Student's *t*-test (Origin Pro SR4 v8. 0951). The level of statistical significance was set at $p < 0.05$ and $p < 0.01$. All values are expressed as mean ± SD.

Results

Iron state

Plasma iron levels

The measurement of plasma iron levels revealed a significant increase in iron overload state, compared with values found in the basal condition (Table 1).

Tissue iron levels

We observed a significant increase in hepatic and pancreatic iron levels in mice with iron overload, with respect to iron-adequate mice (Table 1).

Histochemical studies of hemosiderin

To examine the tissue iron distribution, Prussian blue staining for iron was performed in pancreas and liver from iron adequate and overloaded mice.

In iron overloaded mice, abundant hemosiderin was observed in inter- and perilobular connective cells of pancreas (Fig. 3H). In the liver of iron overloaded mice, we observed hemosiderin in cells identified as Kupffer cells on the basis of their cell morphology (Fig. 3L). In pancreas and liver parenchyma of iron-adequate mice, hemosiderin was undetectable (Fig. 3C, G and K).

In order to determine the presence of hemosiderin in DMT1-, prohepcidin- and L-ferritin-positive cells, the tissue sections were processed by immunohistochemical technique followed by Prussian blue staining for iron.

Immunohistochemical studies

DMT1 expression

DMT1 expression in pancreas was assessed to determine its distribution in a state of iron overload. This study showed that DMT1 immunolocalization was particularly limited to pancreatic endocrine tissue (Fig. 1A and B). In iron-adequate mice the marked DMT1 expression was found mainly in islet of Langerhans cells (Fig. 1A). However, slight DMT1 expression was seen in islet of Langerhans cells in iron overloaded mice compared with the basal state (Fig. 1B).

In the duodenum of iron-adequate mice, DMT1 immunolocalization was mainly cytoplasmic in enterocytes (Fig. 1E). However, in iron overloaded mice, weak DMT1 expression was found in enterocytes with clear perinuclear localization (Fig. 1F), compared with the basal state.

Prohepcidin expression

The study of pancreatic prohepcidin expression in iron-adequate mice revealed that a few cells of Langerhans islet were

Please cite this article in press as: Giorgi G, Roque ME. Iron overload induces changes of pancreatic and duodenal divalent metal transporter 1 and prohepcidin expression in mice. Acta Histochemica (2013), http://dx.doi.org/10.1016/j.acthis.2013.08.013

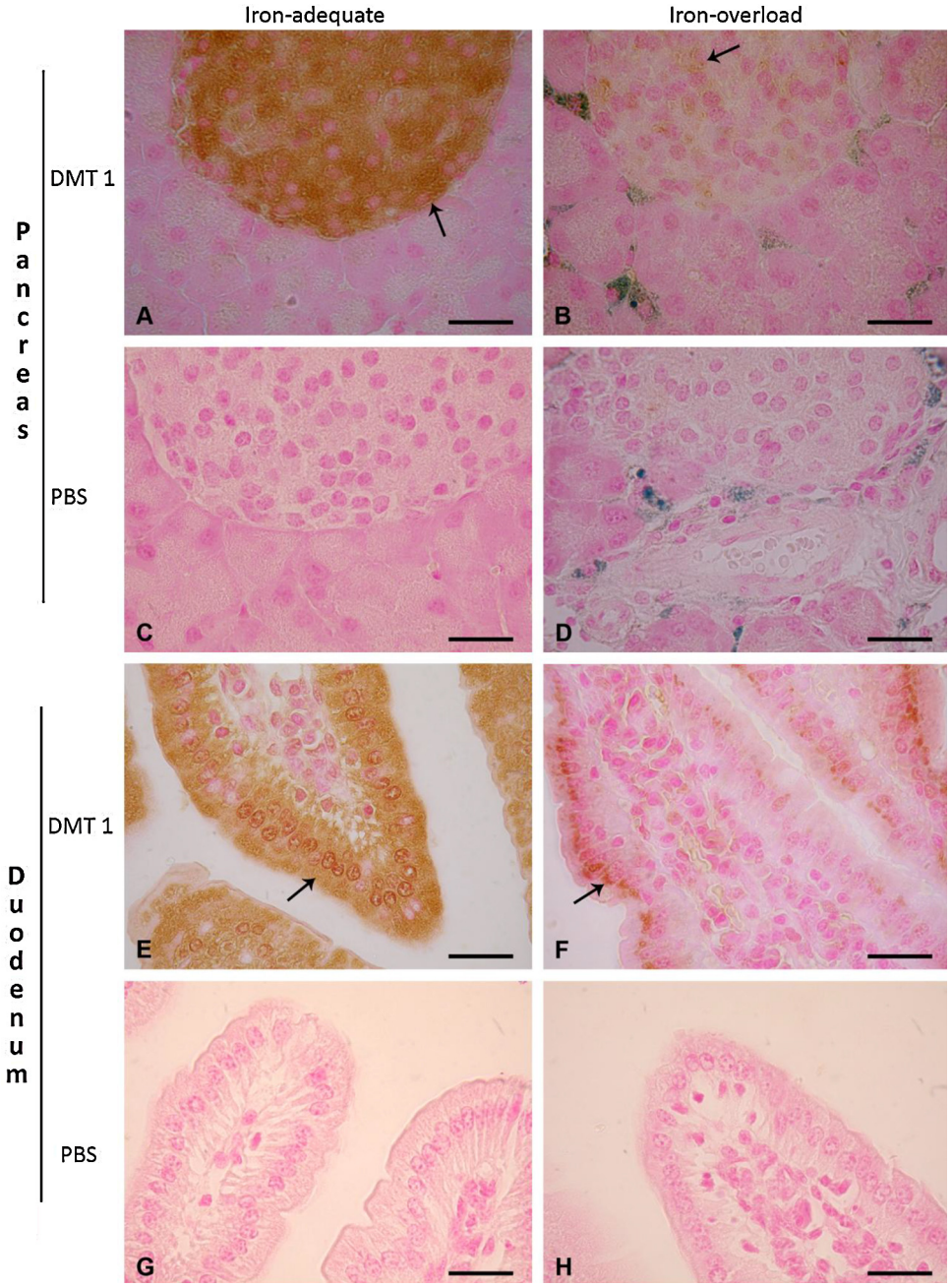

Fig. 1. Immunolocalization of DMT1 in pancreas and duodenum of iron-adequate and overloaded mice. (A) Pancreatic tissue of iron-adequate mice showing marked DMT1 expression in islet of Langerhans cells (arrow). (B) Pancreatic tissue of iron overloaded mice showing slight DMT1 expression in islet of Langerhans cells (arrow). (C) Pancreatic tissue of iron-adequate mice incubated with PBS instead of the primary antibody. Note lack of immunoreactivity. (D) Pancreatic tissue of iron overloaded mice incubated with PBS instead of the primary antibody. Note lack of immunoreactivity. (E) Duodenal tissue of iron-adequate mice showing cytoplasmic DMT1 expression in enterocytes (arrow). (F) Duodenal tissue of iron overloaded mice showing perinuclear DMT1 expression in enterocytes (arrow). (G) Duodenal tissue of iron-adequate mice incubated with PBS instead of the primary antibody. Note lack of immunoreactivity. (H) Duodenal tissue of iron overloaded mice incubated with PBS instead of the primary antibody. Note lack of immunoreactivity. Tissue sections were revealed by DAB in solution followed by Prussian blue iron staining. Scale bars = 20 μm.

positive for this pro-peptide (Fig. 2A). In contrast, a large number of islet cells showed prohepcidin expression in iron overloaded mice (Fig. 2B).

Hepatic prohepcidin expression was particularly marked in hepatocytes associated with central veins and in stroma hepatocytes in iron overloaded mice (Fig. 2F). Nonetheless, in iron-adequate mice, prohepcidin expression was low in hepatocytes associated with central veins (Fig. 2E).

L-ferritin expression

In the pancreas of iron-adequate mice, abundant L-ferritin expression was localized in islets of Langerhans, but it was undetectable in acinar cells (Fig. 3A and E). However, in iron overloaded mice mild L-ferritin staining was found in the islets of Langerhans, but with a marked L-ferritin staining localized in acinar cells and in inter- and perilobular connective tissue cells (Fig. 3B and F).

Please cite this article in press as: Giorgi G, Roque ME. Iron overload induces changes of pancreatic and duodenal divalent metal transporter 1 and prohepcidin expression in mice. Acta Histochemica (2013), http://dx.doi.org/10.1016/j.acthis.2013.08.013

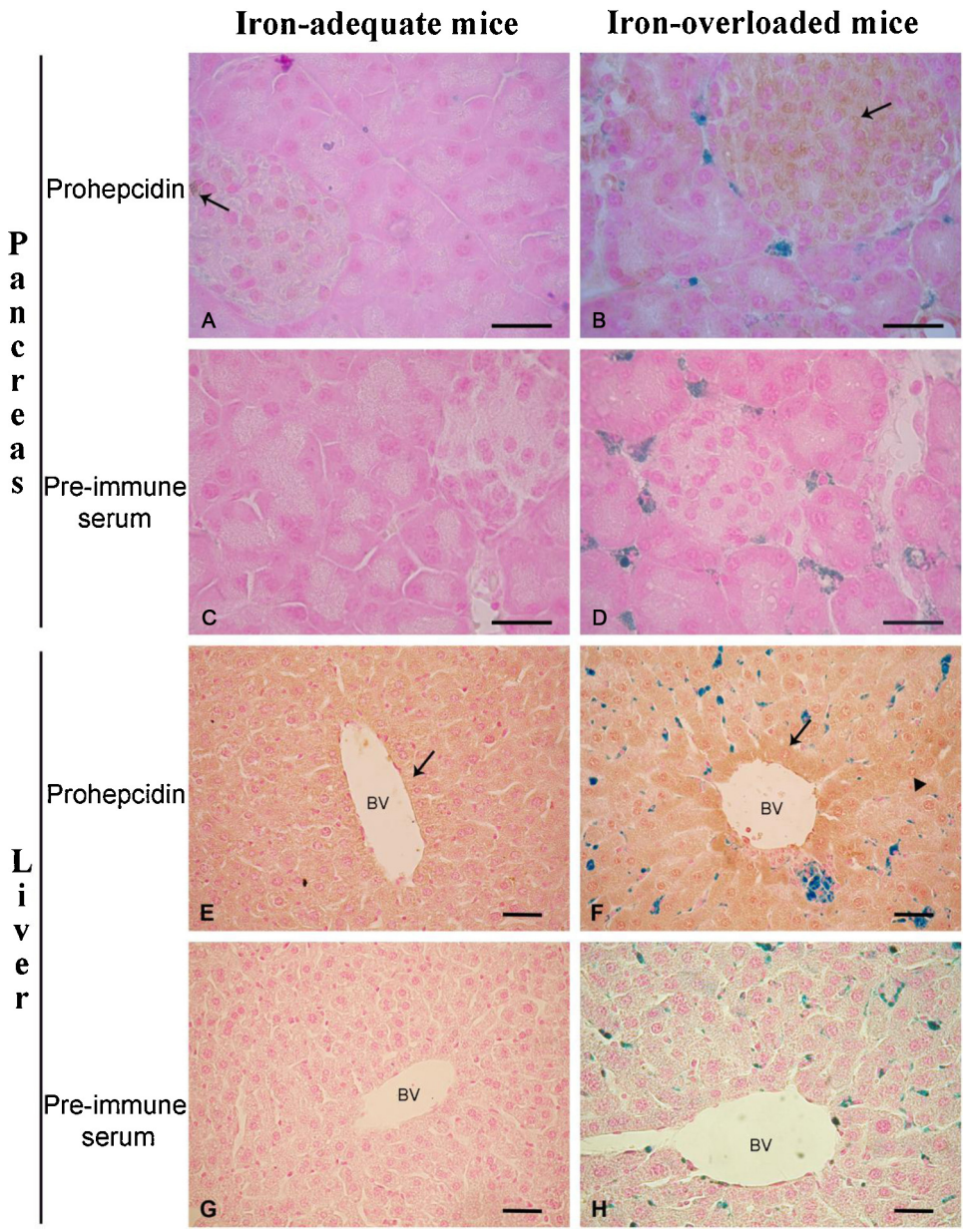

Fig. 2. Immunolocalization of prohepcidin in pancreas and liver of iron-adequate and overloaded mice. (A) Pancreatic tissue of iron-adequate mice showing prohepcidin expression limited to few cells in islet of Langerhans (arrow). (B) Pancreatic tissue of iron overloaded mice showing marked prohepcidin expression in a large number of islet of Langerhans cells (arrow). (C) Pancreatic tissue of iron adequate-mice incubated with pre-immune rabbit serum instead of the primary antibody. Note lack of immunoreactivity. (D) Pancreatic tissue of iron overloaded mice incubated with pre-immune rabbit serum instead of the primary antibody. Note lack of immunoreactivity. (E) Hepatic tissue of iron-adequate mice showing low prohepcidin expression in hepatocytes near blood vessels (arrow). (F) Hepatic tissue of iron overloaded mice showing marked prohepcidin expression in hepatocytes near blood vessels (arrow) and stroma hepatocytes (arrowhead). (G) Hepatic tissue of iron-adequate mice incubated with pre-immune rabbit serum instead of the primary antibody. Note lack of immunoreactivity. (H) Hepatic tissue of iron overloaded mice incubated with pre-immune rabbit serum instead of the primary antibody. Note lack of immunoreactivity. Tissue sections were revealed by DAB in solution followed by Prussian blue iron staining. Blood vessel: BV. Scale bars = 20 μm.

In iron-adequate mice, hepatic L-ferritin immunostaining was mainly in hepatocytes associated with central veins (Fig. 3I). In iron overload state, L-ferritin was localized, not only in hepatocytes surrounding central veins, but also in stroma hepatocytes (Fig. 3J).

Immunoblot analysis of DMT1

To evaluate whether the changes in DMT1 expression by immunohistochemical technique are related to changes in protein content, we examined DMT1 levels in iron adequate and overloaded mice by Western blotting. In agreement with that observed by immunohistochemistry, DMT1 levels were significantly lower in pancreas and duodenum of mice treated with iron, in comparison with iron-adequate mice (Fig. 4A and B). In sections processed as negative controls immunoreactivity was not observed (data not shown).

Hematological data

Baseline hematology data

Basal hemoglobin and hematocrit values were 14.2 ± 0.7 g/dL and $49 \pm 1\%$, respectively.

Please cite this article in press as: Giorgi G, Roque ME. Iron overload induces changes of pancreatic and duodenal divalent metal transporter 1 and prohepcidin expression in mice. Acta Histochemica (2013), http://dx.doi.org/10.1016/j.acthis.2013.08.013

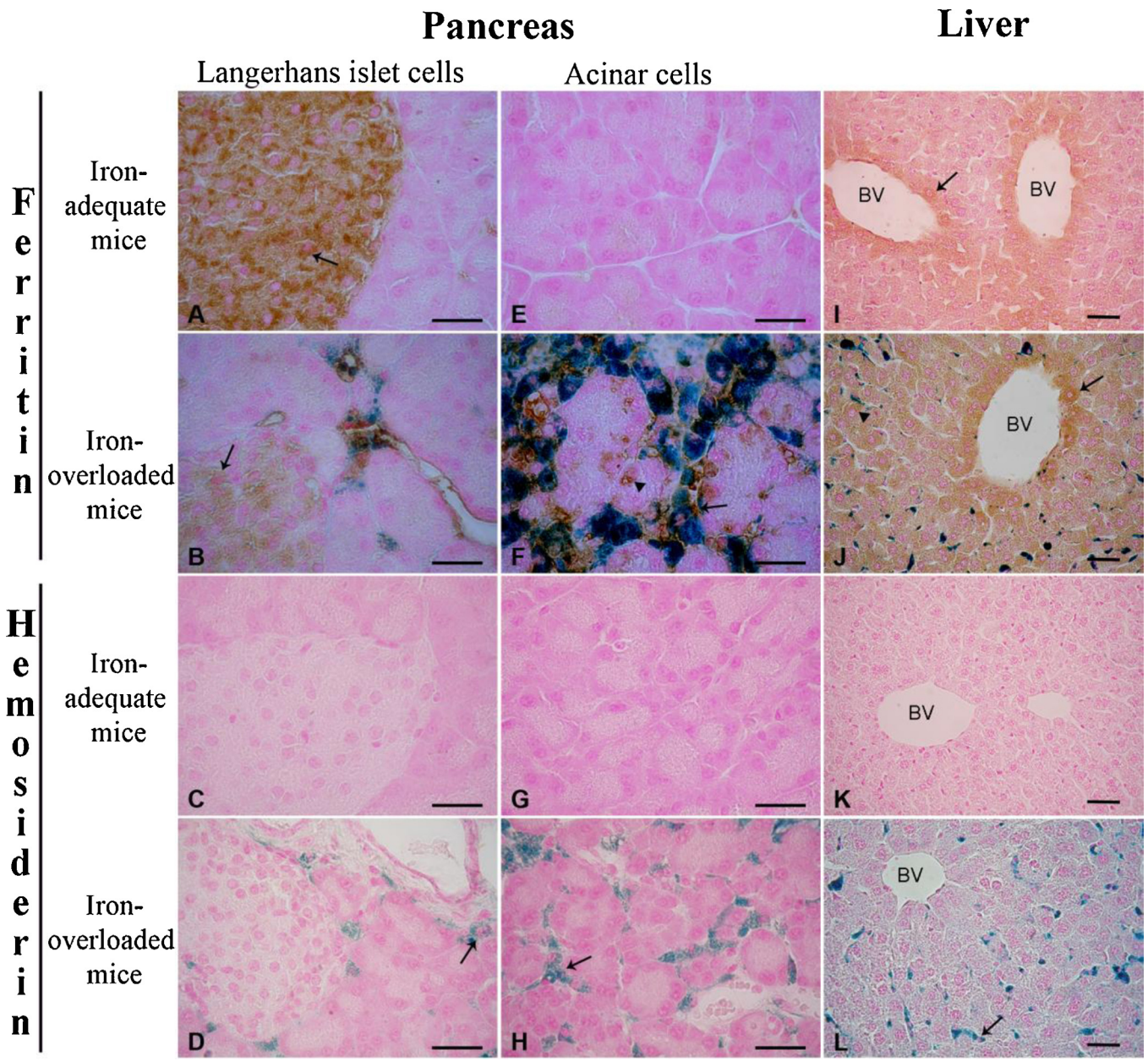

Fig. 3. Immunolocalization of ferritin and histochemical study in pancreas and liver of iron adequate and overloaded mice. (A) Pancreatic tissue of iron-adequate mice showing marked ferritin expression in islet of Langerhans cells (arrow). (B) Pancreatic tissue of iron overloaded mice showing low ferritin expression in islets of Langerhans (arrow). (C) Hemosiderin in pancreatic tissue of iron-adequate mice was undetectable in islets of Langerhans. (D) Hemosiderin in pancreatic tissue of iron overloaded mice was undetectable in islets of Langerhans. (E) Pancreatic tissue of iron-adequate mice showing undetectable ferritin expression in acinar cells. (F) Pancreatic tissue of iron overloaded mice showing ferritin expression in acinar cells (arrowhead) and in inter- and perilobular connective tissue cells (arrow). (G) Hemosiderin in pancreatic tissue of iron-adequate mice was undetectable in acinar cells and in inter- and perilobular connective tissue cells. (H) Hemosiderin in pancreatic tissue of iron overloaded mice was detectable in inter- and perilobular connective tissue cells (arrow). (I) Hepatic tissue of iron-adequate mice showing low ferritin expression in hepatocytes near blood vessels (arrow). (J) Hepatic tissue of iron overloaded mice showing marked ferritin expression in hepatocytes near blood vessels (arrow) and stroma hepatocytes (arrowhead). (K) Hemosiderin in hepatic tissue of iron-adequate mice was undetectable. (L) Hemosiderin in hepatic tissue of iron overloaded mice was detectable in cells identified as Kupffer cells on the basis of their cell morphology (arrow). Tissue sections for immunohistochemistry were revealed by DAB in solution followed by Prussian blue iron staining. Prussian blue iron staining was used to determine hemosiderin. Blood vessel: BV. Scale bars = 20 μm.

Iron adequate and overload hematology data

Hemoglobin levels were lower in iron overloaded mice (14.1 ± 0.6 g/dL), compared with iron-adequate mice (15.6 ± 0.2 g/dL). A similar change was observed in hematocrit in iron overload state ($44 \pm 1\%$) with respect to basal state ($49 \pm 1\%$).

Discussion

The present study reports that DMT1 is expressed mainly in the islets of Langerhans, in both iron adequate and overloaded mice. In agreement with another report we demonstrated a clear DMT1 expression in iron adequate mice in islets of Langerhans in pancreatic parenchyma (Koch et al., 2003). Our data strongly indicate that iron overload induced a dramatic decrease of DMT1 expression in endocrine cells, showing that DMT1 was down-regulated in islets of Langerhans cells of iron overloaded mice.

The molecular mechanisms that mediate the uptake of cellular iron in the pancreas remain poorly defined. Therefore, in order to elucidate the iron cycle in pancreas we analyzed functional relations between DMT1 and pancreatic prohepcidin, the well-known

Please cite this article in press as: Giorgi G, Roque ME. Iron overload induces changes of pancreatic and duodenal divalent metal transporter 1 and prohepcidin expression in mice. Acta Histochemica (2013), http://dx.doi.org/10.1016/j.acthis.2013.08.013

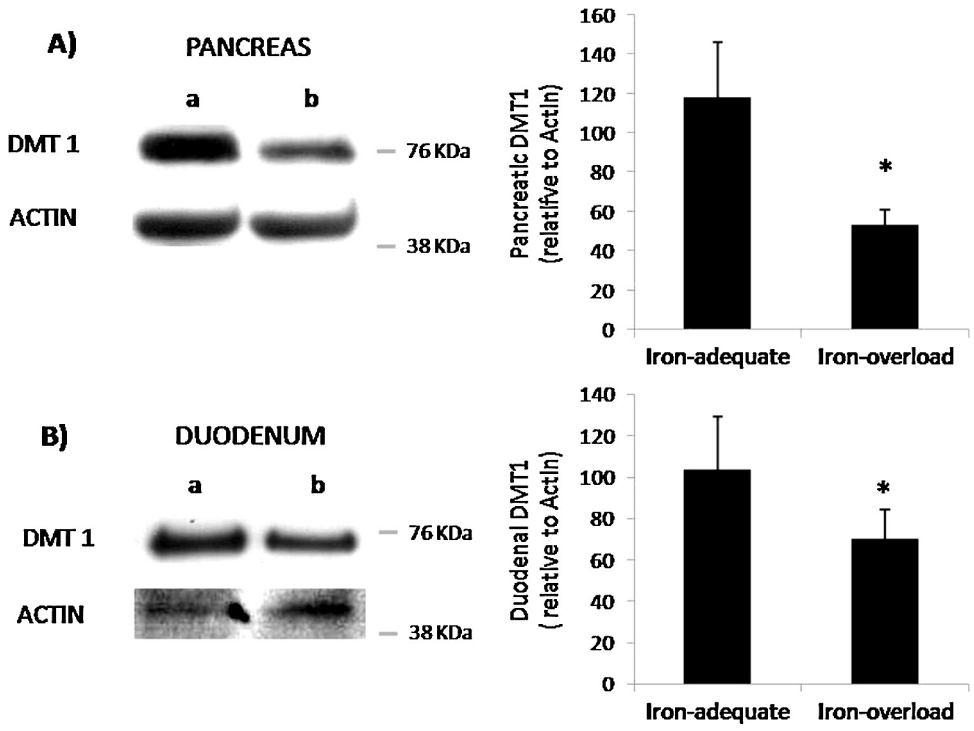

Fig. 4. Immunoblot of divalent metal transporter (DMT1) in pancreas and duodenum. The sizes (in kDa) of the molecular mass markers are indicated on the right of the blot. (A) Immunoblotting analysis of pancreatic DMT1; (B) immunoblotting analysis of duodenal DMT1. (a) Iron-adequate mice; (b) iron overloaded mice ($n = 3$). The graphs represent the quantification of the densitometric scans of the western blot data. Tissue were processed as described in Materials and Methods section. $^{*}p \leq 0.05$ iron-adequate mice *vs.* iron overloaded mice. The data shown are representative.

propeptide that it converts into the main regulator of cellular and systemic iron in most tissues, called hepcidin.

Valore and Ganz (2008) have reported that the hepatic convertase furin mediates the post-translational processing of hepcidin and that the proteolytic cleavage of prohepcidin gives hepcidin that is secreted to blood plasma. Studies by Lee and Beutler (2009) reported the hepatic hepcidin transcriptional regulation by iron, erythropoietic activity and inflammation, and other study demonstrated the increase of prohepcidin when hepcidin expression is stimulated (Valore and Ganz, 2008). In fact, since there is no evidence yet of other type of control, the hepcidin levels are well correlated with tissue prohepcidin expression (Flanagan et al., 2007).

In agreement with the study of Kulaksiz et al. (2008), we detected prohepcidin in pancreatic islet cells in basal conditions. An important finding of our study was the immunohistochemical detection of a clear increase of prohepcidin expression in iron excess in islets of Langerhans cells. Interestingly, in most endocrine cells of islets of Langerhans prohepcidin was expressed. The number of hepatocytes that expressed prohepcidin, was also higher in iron overload than in iron adequate mice (D'Anna and Roque, 2013). These findings allow us to propose a similar regulation of hepcidin in pancreas and liver by iron. It is well known that endocrine cells secrete their molecules into the blood. In this sense, we would suggest that pancreatic hepcidin may have a local role in iron regulation and also could contribute to the systemic pool. This finding is in agreement with the study of Kulaksiz et al. (2008), who observed that hepcidin expression in rat insulinoma cells was up-regulated by iron.

The possible role of iron stores of pancreatic endocrine cells could be suggested by the presence of high ferritin expression in iron adequate mice detected by immunohistochemical studies. This finding is in accordance with MacDonald et al. (1994) in islets of Langerhans cells in basal conditions. The high ferritin expression detected in endocrine cells may be explained by high iron fluxes through the increased DMT1 expression in basal condition (Kulaksiz et al., 2008). In iron overloaded mice, the decrease of ferritin expression in islet cells could be explained by the reduced iron uptake as a consequence of the decrease of DMT1 expression that we demonstrated. As a result, the lack of hemosiderin in islets of Langerhans was expected.

In contrast, studies of Lu et al. (1991) reported an increase of ferritin and hemosiderin in endocrine cells using Fe^{3+}-NTA. These discrepancies could be due to different iron types used to induce iron overload, as reported Awai et al. (1979). These authors have been clearly showed hemosiderin pigments in islet cells of iron overloaded rats with Fe^{3+}-NTA, but not when colloidal iron was used.

In addition, the iron saccharate is a colloidal iron that is taken up by macrophages of the reticuloendothelial system, where iron is released from the iron carbohydrate compound into an iron pool. Later, iron is either incorporated by ferritin or is released from the cell (Danielson, 2004). Taking all together, the pattern of iron accumulation depends on the type of iron used, thus the nature of the iron could explain the hemosiderin deposits in reticuloendothelial cells that we demonstrated.

On the other hand, when we analyzed iron storage in the exocrine pancreas, the strong iron stores found in peri- and interlobular connective cells and acinar cells in iron excess state, could indicate that the pancreatic exocrine and connective tissue participate in iron storage. Finally, our findings could suggest that the exocrine pancreas has a similar function to the liver, which is well known to store excess iron (Graham et al., 2007). According to our results, this pattern of iron distribution was also found by other authors (Awai et al., 1979; Iancu et al., 1987). Interestingly, the absence of DMT1 expression in acinar cells where iron stores founded could indicate that DMT1 is not the main iron uptake pathway in these cells.

Please cite this article in press as: Giorgi G, Roque ME. Iron overload induces changes of pancreatic and duodenal divalent metal transporter 1 and prohepcidin expression in mice. Acta Histochemica (2013), http://dx.doi.org/10.1016/j.acthis.2013.08.013

Regarding these conclusions, recent studies reported that ZIP14 takes up not only NTBI, but also iron-bound to transferrin *via* endocytosis in pancreatic acinar cells (Zhao et al., 2010; Nam et al., 2013). Based on the findings of Nam et al. (2013), who reported that ZIP14 is up-regulated in acinar cells by iron excess, we could explain that the ferritin expression in acinar cells may be due to the presence of another importer, such as ZIP14, since DMT1 is not expressed in these cells. Indeed, in contrast to our results, these authors showed that pancreatic DMT1 levels were not affected by iron status. However, it is difficult to compare both studies by the different procedures carried out in each case, since we used colloidal iron form instead of enriched diets.

Taking into account the inverse relationship determined in the present study between pancreatic DMT1 and hepcidin in iron excess, it is worth noting the importance of evaluating the relationship between duodenal DMT1 and hepcidin which has been well studied in most tissues. In fact, in accordance with Núñez et al. (2010), we found that duodenal DMT1 levels were lower in iron overloaded animals than in iron adequate.

Our findings allow us to propose a similar regulation of DMT1 expression in pancreatic islet cells and duodenum by the pattern of DMT1 expression and its inverse relationship with hepcidin in both tissues. These results could indicate that in iron overload, DMT1 and hepcidin in islet cells act in a coordinated manner similar to that reported in duodenal tissue (Mena et al., 2008; Chung et al., 2009; Brasse-Lagnel et al., 2011). It will therefore be necessary to carry out further studies to determine the regulatory mechanisms at work between DMT1 and hepcidin in islets of Langerhans.

On the other hand, the cytoplasmic redistribution of DMT1 toward the perinuclear zone in enterocytes could indicate low iron uptake of duodenal cells during iron overload. Although this localization is different to that observed by Núñez et al. (2010), both studies indicate a reduced iron duodenal uptake, in accordance with a lower DMT1 expression reported in these two studies. This could support our proposal of the regulatory interrelationship between hepcidin and DMT1.

Finally we can conclude that our findings indicate that pancreatic and duodenal DMT1 are down-regulated in iron overload. In addition, the increased synthesis of hepcidin in islets of Langerhans by iron excess could negatively regulate pancreatic DMT1. This behavior is associated with the reduced ferritin expression in the islets of Langerhans. Therefore, further studies will be necessary to determine the regulatory mechanisms between hepcidin and DMT1 in pancreas, as well as other proteins that are involved.

Taken together, the marked decrease of DMT1, the increase of hepcidin and the reduction of ferritin in pancreatic endocrine tissue induced by iron overload could explain that in islets of Langerhans, DMT1 is down-regulated by high hepcidin expression through an autocrine and endocrine mechanism. These hypotheses may indicate one of several mechanisms that may operate simultaneously in the pancreas in diseases involving iron excess.

Acknowledgments

This research was supported by the Secretaría General de Ciencia y Tecnología de la Universidad Nacional del Sur (Grant 24/B116). We are very grateful to Doctor François Canonne-Hergaux for generously providing DMT1 antibody reagents, and Doctors Paolo Santambrogio and Tomas Ganz for providing ferritin and prohepcidin antibody reagents. We are grateful to Dr. Alejandro Curino and his lab group.

References

Andrews NC. The iron transporter DMT1. Int J Biochem Cell Biol 1999;31:991–4.

Awai M, Narasaki M, Yamanoi Y, Seno S. Induction of diabetes in animals by parenteral administration of ferric nitrilotriacetate. Am J Pathol 1979;95:663–74.

Brasse-Lagnel C, Karim Z, Letteron P, Bekri S, Bado A, Beaumont C. Intestinal DMT1 cotransporter is down-regulated by hepcidin via proteasome internalization and degradation. Gastroenterology 2011;140:1261–71.

Beutler E. Hemochromatosis: genetics and pathophysiology. Annu Rev Med 2006;57:331–47.

Bradford MM. A rapid and sensitive method for the quantitation of microgram quantities of protein utilizing the principle of protein-dye binding. Anal Biochem 1976;72:248–54.

Canonne-Hergaux F, Gruenheid S, Ponka P, Gros P. Cellular and subcellular localization of the Nramp2 iron transporter in the intestinal brush border and regulation by dietary iron. Blood 1999;93:4406–17.

Chung B, Chaston T, Marks J, Srai SK, Sharp PA. Hepcidin decreases iron transporter expression in vivo in mouse duodenum and spleen and in vitro in THP-1 macrophages and intestinal Caco-2 cells. J Nutr 2009;139:1457–62.

Committee on Care and Use of Laboratory Animals. Guide on Care and Use of Laboratory Animals. Washington, DC: NIH Publications; 1996 [(Natl. Inst Health, Bethesda) No. 86-23 (DRR/NIH)].

D'Anna MC, Giorgi G, Roque ME. Immunohistochemical studies on duodenum, spleen and liver in mice: distribution of ferroportin and prohepcidin in an inflammation model. Int J Morphol 2011;29:747–53.

D'Anna MC, Roque ME. Physiological focus on the erythropoietin–hepcidin–ferroportin axis. Can J Physiol Pharmacol 2013., http://dx.doi.org/10.1189/cjpp-2012-0214.

D'Anna MC, Veuthey TV, Roque ME. Immunolocalization of ferroportin in healthy and anemic mice. J Histochem Cytochem 2009;57:9–16.

Danielson BG. Structure, chemistry, and pharmacokinetics of intravenous iron agents. J Am Soc Nephrol 2004;15:S93–8.

De Domenico I, Ward MD, Kaplan J. Hepcidin and ferroportin: the new players in iron metabolism. Semin Liver Dis 2011;31:272–9.

Finberg KE. Unraveling mechanisms regulating systemic iron homeostasis. Hematol Am Soc Hematol Educ Program 2011;2011:532–7.

Flanagan JM, Truksa J, Peng H, Lee P, Beutler E. In vivo imaging of hepcidin promoter stimulation by iron and inflammation. Blood Cells Mol Dis 2007;38:253–7.

Ganz T, Nemeth E. Iron imports IV. Hepcidin and regulation of body iron metabolism. Am J Physiol Gastrointest Liver Physiol 2006;290:G199–203.

Gkouvatsos K, Papanikolaou G, Pantopoulos K. Regulation of iron transport and the role of transferrin. Biochim Biophys Acta 2012;1820:188–202.

Graham RM, Chua AC, Herbison CE, Olynyk JK, Trinder D. Liver iron transport. World J Gastroenterol 2007;13:4725–36.

Iancu TC. Ultrastructural aspects of iron storage, transport and metabolism. J Neural Transm 2011;118:329–35.

Iancu TC, Ward RJ, Peters TJ. Ultrastructural observations in the carbonyl iron-fed rat, an animal model for hemochromatosis. Virchows Arch B 1987;53:208–17.

Koch RO, Zoller H, Theurl I, Obrist P, Egg G, Strohmayer W, et al. Distribution of DMT1 within the human glandular system. Histol Histopathol 2003;18:1095–101.

Kulaksiz H, Fein E, Redecker P, Stremmel W, Adler G, Cetin Y. Pancreatic *b*-cells express hepcidin, an iron-uptake regulatory peptide. J Endocrinol 2008;197:241–9.

Lee PL, Beutler E. Regulation of hepcidin and iron-overload disease. Annu Rev Pathol Mech Dis 2009;4:489–515.

Please cite this article in press as: Giorgi G, Roque ME. Iron overload induces changes of pancreatic and duodenal divalent metal transporter 1 and prohepcidin expression in mice. Acta Histochemica (2013), http://dx.doi.org/10.1016/j.acthis.2013.08.013

Lu JP, Hayashi K, Okada S, Awai M. Transferrin receptors and selective iron deposition in pancreatic B cells of iron-overloaded rats. Acta Phatol Japon 1991;41:647–52.

MacDonald MJ, Cook JD, Epstein ML, Flowers CH. Large amount of (apo)ferritin in the pancreatic insulin cell and its stimulation by glucose. FASEB J 1994;8:777–81.

Masaratana P, Laftah AH, Latunde-Dada GO, Vaulont S, Simpson RJ, McKie AT. Iron absorption in hepcidin1 knockout mice. Br J Nutr 2011;105:1583–91.

Mastrogiannaki M, Matak P, Keith B, Simon MC, Vaulont S, Peyssonnaux C. HIF-2alpha, but not HIF-1alpha, promotes iron absorption in mice. J Clin Invest 2009;119:1159–66.

Mena NP, Esparza A, Tapia V, Valdés P, Núñez MT. Hepcidin inhibits apical iron uptake in intestinal cells. Am J Physiol Gastrointest Liver Physiol 2008;294:G192–8.

Nam H, Wang CY, Zhang L, Zhang W, Hojyo S, Fukada T, et al. ZIP14 and DMT1 in the liver, pancreas, and heart are differentially regulated by iron deficiency and overload: implications for tissue iron uptake in iron-related disorders. Haematologica 2013;98:1049–57.

Nemeth E, Tuttle MS, Powelson J, Vaughn MB, Donovan A, Ward DM, et al. Hepcidin regulates cellular iron efflux by binding to ferroportin and inducing its internalization. Science 2004;306:2090–3.

Nicolas G, Bennoun M, Devaux I, Beaumont C, Grandchamp B, Kahn A, et al. Lack of hepcidin gene expression and severe tissue iron overload in upstream stimulatory factor 2 (USF2) knockout mice. Proc Natl Acad Sci USA 2001;98:8780–5.

Núñez MT, Tapia V, Rojas A, Aguirre P, Gómez F, Nualart F. Iron supply determines apical/basolateral membrane distribution of intestinal iron transporters DMT1 and ferroportin 1. Am J Physiol Cell Physiol 2010;298:C477–85.

Oyarzabal MI, Rabasa SL. Riqueza genética y estabilidad en ratones de la cepa CF1. Mendeliana 1999;13:74–84.

Park CH, Valore EV, Waring AJ, Ganz T. Hepcidin, a urinary antimicrobial peptide synthesized in the liver. J Biol Chem 2001;276:7806–10.

Ramey G, Faye A, Durel B, Viollet B, Vaulont S. Iron overload in Hepc1−/− mice is not impairing glucose homeostasis. FEBS Lett 2007;581:1053–7.

Santambrogio P, Cozzi A, Levi S, Rovida E, Magni F, Albertini A, et al. Functional and immunological analysis of recombinant mouse H- and L-Ferritins from *Escherichia coli*. Protein Expr Purif 2000;19:212–8.

Trinder D, Oates PS, Thomas C, Sadleir J, Morgan EH. Localisation of divalent metal transporter 1 (DMT1) to the microvillus membrane of rat duodenal enterocytes in iron deficiency, but to hepatocytes in iron overload. Gut 2000;46:270–6.

Vanoaica L, Darshan D, Richman L, Schümann K, Kühn LC, Intestinal Ferritin H. Is required for an accurate control of iron absorption. Cell Metab 2010;12:273–82.

Valore EV, Ganz T. Posttranslational processing of hepcidin in human hepatocytes is mediated by the prohormone convertase furin. Blood Cells Mol Dis 2008;40:132–8.

Veuthey T, D'Anna MC, Roque ME. Role of the kidney in iron homeostasis: renal expression of prohepcidin, ferroportin, and DMT1 in anemic mice. Am J Physiol Renal Physiol 2008;295:1213–21.

Zhao N, Gao J, Enns CA, Knutson MD. ZRT/IRT-like protein 14 (ZIP14) promotes the cellular assimilation of iron from transferrin. J Biol Chem 2010;285:32141–50.

Please cite this article in press as: Giorgi G, Roque ME. Iron overload induces changes of pancreatic and duodenal divalent metal transporter 1 and prohepcidin expression in mice. Acta Histochemica (2013), http://dx.doi.org/10.1016/j.acthis.2013.08.013